Phase-amplitude coupled persistent theta and gamma oscillations in rat primary motor cortex *in vitro*

Nicholas W. Johnson [a], Mazhar Özkan [b], Adrian P. Burgess [a], Emma J. Prokic [a], Keith A. Wafford [c], Michael J. O'Neill [c], Stuart D. Greenhill [a], Ian M. Stanford [a], Gavin L. Woodhall [a, *]

[a] Aston Brain Centre, Aston University, School of Life and Health Sciences, Birmingham, B4 7ET, United Kingdom
[b] Department of Anatomy, School of Medicine, Marmara University, Istanbul, Turkey
[c] Neuroscience Division, Eli Lilly & Co. Ltd., Windlesham, GU20 6PH, United Kingdom

A B S T R A C T

In vivo, theta (4–7 Hz) and gamma (30–80 Hz) neuronal network oscillations are known to coexist and display phase-amplitude coupling (PAC). However, *in vitro*, these oscillations have for many years been studied in isolation. Using an improved brain slice preparation technique we have, using co-application of carbachol (10 μM) and kainic acid (150 nM), elicited simultaneous theta (6.6 ± 0.1 Hz) and gamma (36.6 ± 0.4 Hz) oscillations in rodent primary motor cortex (M1). Each oscillation showed greatest power in layer V. Using a variety of time series analyses we detected significant cross-frequency coupling in 74% of slice preparations.

Differences were observed in the pharmacological profile of each oscillation. Thus, gamma oscillations were reduced by the GABA$_A$ receptor antagonists, gabazine (250 nM and 2 μM), and picrotoxin (50 μM) and augmented by AMPA receptor antagonism with SYM2206 (20 μM). In contrast, theta oscillatory power was increased by gabazine, picrotoxin and SYM2206. GABA$_B$ receptor blockade with CGP55845 (5 μM) increased both theta and gamma power, and similar effects were seen with diazepam, zolpidem, MK801 and a series of metabotropic glutamate receptor antagonists. Oscillatory activity at both frequencies was reduced by the gap junction blocker carbenoxolone (200 μM) and by atropine (5 μM).

These data show theta and gamma oscillations in layer V of rat M1 *in vitro* are cross-frequency coupled, and are mechanistically distinct. The development of an *in vitro* model of phase-amplitude coupled oscillations will facilitate further mechanistic investigation of the generation and modulation of coupled activity in mammalian cortex.

© 2017 The Authors. Published by Elsevier Ltd. This is an open access article under the CC BY-NC-ND license (http://creativecommons.org/licenses/by-nc-nd/4.0/).

1. Introduction

Gamma oscillations (30–80 Hz) play a role in attentive states such as sensory perception (Engel and Singer, 2001; Gray et al., 1989; Gray, 1994; Singer and Gray, 1995), memory processing (Chrobak and Buzsáki, 1998; Lisman and Idiart, 1995) and movement execution (Brown et al., 1998; Cheyne et al., 2008; Muthukumaraswamy, 2010; Pfurtscheller et al., 2003). Extensively studied both *in vivo* and *in vitro*, gamma oscillations appear to be an emergent property of reciprocally connected inhibitory interneuronal network and pyramidal cells. Whilst excitatory postsynaptic potentials, shunting inhibition and gap junctions play a role in the generation of synchronous activity, the main determinant of the oscillatory frequency is the time constant of decay of interneuron-derived GABA currents (Fisahn et al., 1998; Traub et al., 1996, 2000; Wang and Buzsáki, 1996; Whittington et al., 1995).

Theta oscillations (4–7 Hz) are associated with hippocampal and limbic regions involved in exploration, spatial navigation (Cacucci et al., 2004; O'Keefe and Recce, 1993) and spatial and working memory (Buzsáki and Moser, 2013; Cashdollar et al., 2009). During exploration, network oscillations at gamma and

theta frequency are often co-generated (Bragin et al., 1995) with theta being temporally nested with gamma rhythm (Fisahn et al., 1998; Sirota et al., 2008). Due to conduction delays, low frequency oscillations are able to prefentially synchronise networks over long distances while faster oscillations are thought to synchronise activity in more local networks. Thus, the amplitude of the gamma frequency oscillation is enhanced in phase with the theta cycle due to neuron recruitment. This phenomenon, known as cross-frequency coupling (CFC; Canolty et al., 2006), aids interneuronal network communication and processing such that communications arriving out of phase may be ignored while information in phase may be treated preferentially. In this way, theta may serve to act as a global temporal coordinator of local network activity (Sirota et al., 2008), and theta-gamma coupling has been shown to be essential for structuring of motor-related activity in rodent M1 (Igarashi et al., 2013).

An understanding of the fundamental mechanisms involved in the generation of neuronal network theta and gamma oscillations has arisen from *in vitro* studies using stimulus-based and/or pharmacological approaches to induce activity, which may then be characterised using a combination of electrophysiology and neuropharmacology. Thus, transient (lasting milliseconds to seconds) gamma oscillations have been evoked by tetanic electrical stimulation (Traub et al., 1996; Whittington et al., 1997) whilst persistent (lasting hours) gamma oscillations have been generated by application of kainic acid (KA) and/or carbachol (CCh) (Buhl et al., 1998; Cunningham et al., 2003; Dickson et al., 2000; Fisahn et al., 1998) or group 1 metabotropic glutamate receptor (mGluR) activation (Fisahn et al., 1998; Pálhalmi et al., 2004; Whittington et al., 1995). Furthermore, theta rhythms can be generated by the addition of GABA$_A$ receptor antagonists along with CCh (Konopacki and Golebiewski, 1993; Lukatch and MacIver, 1997; MacIver et al., 1986) or AMPA receptor antagonists with mGluR agonists (Cobb et al., 2000; Gillies et al., 2002). In addition, rhythm generation is also enhanced by electrical coupling through gap junctions (Bocian et al., 2011; Kopell and Ermentrout, 2004; Szabadics et al., 2001; Tamas et al., 2000) which are prevalent between interneurons (Beierlein et al., 2000; Deans et al., 2001; Galarreta and Hestrin, 1999).

Previous studies in M1 *in vitro* have shown that co-application of KA and CCh elicits beta oscillations (Lacey et al., 2014; Yamawaki et al., 2008) while electrical stimulation at different frequencies evoked theta, beta and gamma activity revealing the ability for M1 to promote multiple rhythms of different frequencies (Yamawaki et al., 2008). In this study, using an improved brain slice preparation based on a protocol utilising a number of neuroprotective agents, we have been able to generate pharmacologically-induced persistent theta and gamma oscillations in M1 that demonstrates CFC. Furthermore, pharmacological investigations reveal that theta activity is generated and modulated by distinct receptor types, with contributions from both intrinsic and synaptic mechanisms.

2. Materials and methods

2.1. In vitro slice preparation

Sagittal brain slices (450 μm thick) containing M1 were prepared from male Wistar rats (20–30 days of age, 50–150 g). All animal procedures were performed in accordance with the Aston University policy and in accordance with the Animals (Scientific Procedures) Act UK 1986 and European Communities Directive 2010/63/EU. Animals were first anaesthetised using isoflurane (2% in O$_2$) until no heartbeat was detected and then transcardially perfused with ice-cold sucrose-based artificial cerebral spinal fluid (aCSF) containing (in mM): 180 sucrose, KCl 2.5, MgSO$_4$ 10,

NaH$_2$PO$_4$ 1.25, NaHCO$_3$ 25 Glucose 10, CaCl$_2$ 0.5, ascorbic acid 1, N-acetyl cysteine 2, taurine 1, Ethyl pyruvate 20 and saturated with 95% O$_2$ and 5% CO$_2$ at pH 7.3, 300–310 mOsm. Indomethacin (45 μM), aminoguanidine (200 μM) and uric acid (400 μM) were added to improve slice viability (Griffiths et al., 1993; Pakhotin et al., 1997; Proctor, 2008). The brain was quickly removed and placed into the same sucrose-based aCSF. Using a HM-650V Microslicer (Microm GMBH, Germany) sagittal slices were cut at room temperature. Slices were then transferred to an interface holding chamber at room temperature containing oxygenated standard aCSF containing (in mM): NaCl 126, KCl 3, MgSO$_4$ 1.6, NaH$_2$PO$_4$ 1.25, NaHCO$_3$ 26, glucose 10, CaCl$_2$ 2 with an osmolarity between 300 and 310 mOsm, where they were left for at least 1 h.

2.2. Extracellular recordings

Slices were transferred to an interface recording chamber (Scientific System Design Inc., Canada) at 32–34 °C and continually perfused at 1–2 ml/min with standard aCSF. Local field potential (LFP) recordings were made using borosilicate glass microelectrodes pulled on a Flaming-Brown micropipette puller (P-2000; Sutter Instrument Co., USA) filled with standard aCSF (resistance of 1–3 MΩ). For cross-correlation recordings, electrodes were placed in a single slice (in layers II/III, Va and Vb), in a single vertical column and recorded for at least 20 min. Signals were amplified 1000-fold using an EXT10-2F amplifier and an LHBF-48X filter (NPI Electronics GMBH, Germany), high- and low-pass filtered at 0.5 Hz and 700 Hz respectively. Low amplitude 50 Hz signal interference was removed using a HumBug (Quest Scientific, North Vancouver, Canada). Signals were digitized and recorded at 10 kHz using a CED micro-1401 mkII digitizer and Spike2 software (Cambridge Electronic Design, UK) and saved to disk.

2.3. Drug application

Oscillatory activity was induced through bath application of KA (150 nM) and CCh (10 μM) and left to stabilise for at least 60 min prior to recording. Drugs were bath applied in known concentrations having been previously prepared in stock solutions of 1–50 mM and stored at −20 °C prior to application. The drugs used were carbamoylcholine chloride (carbachol), carbenoxolone, diazepam, zolpidem, atropine (Sigma Ltd., Gillingham, UK), kainic acid, CPCCOEt, gabazine, MPEP hydrochloride (Abcam, Cambridge, UK) and CGP58845, LY341495, MK-801, picrotoxin and SYM2206 (Tocris Bioscience, Bristol, UK). All drugs were left for at least 40 min before data was sampled or next dose was applied, with the exception of carbenoxolone which was applied for at least 90 min.

2.4. Data analysis

Data were analysed off-line using Spike2 (CED, UK). Raw data presented were filtered using IIR digital filtering by Bessel band pass between 3 and 10 Hz for theta oscillations and 30–45 Hz for gamma oscillations and were forward and reverse filtered using a custom Matlab script in order to preserve phase information. Some data (presented in Fig. 1Ai) were filtered using IIR digital filtering by Bessel low-pass at 60 Hz. Time-frequency profiles were generated using a Morlet-wavelet time-frequency analysis over the 0.5–50 Hz range in frequency bins of 0.5 Hz. Cross- and auto-correlation graphs were generated in Spike2 and referenced to the electrode in LVa. These were presented over 0.2 s for theta oscillations and 0.02 s for gamma oscillations. Results were pooled from 6 recordings to provide a mean result ± SEM. Changes to power values were derived from power spectra generated with Fourier analysis on digitized data of 40 s epochs of recorded activity from control
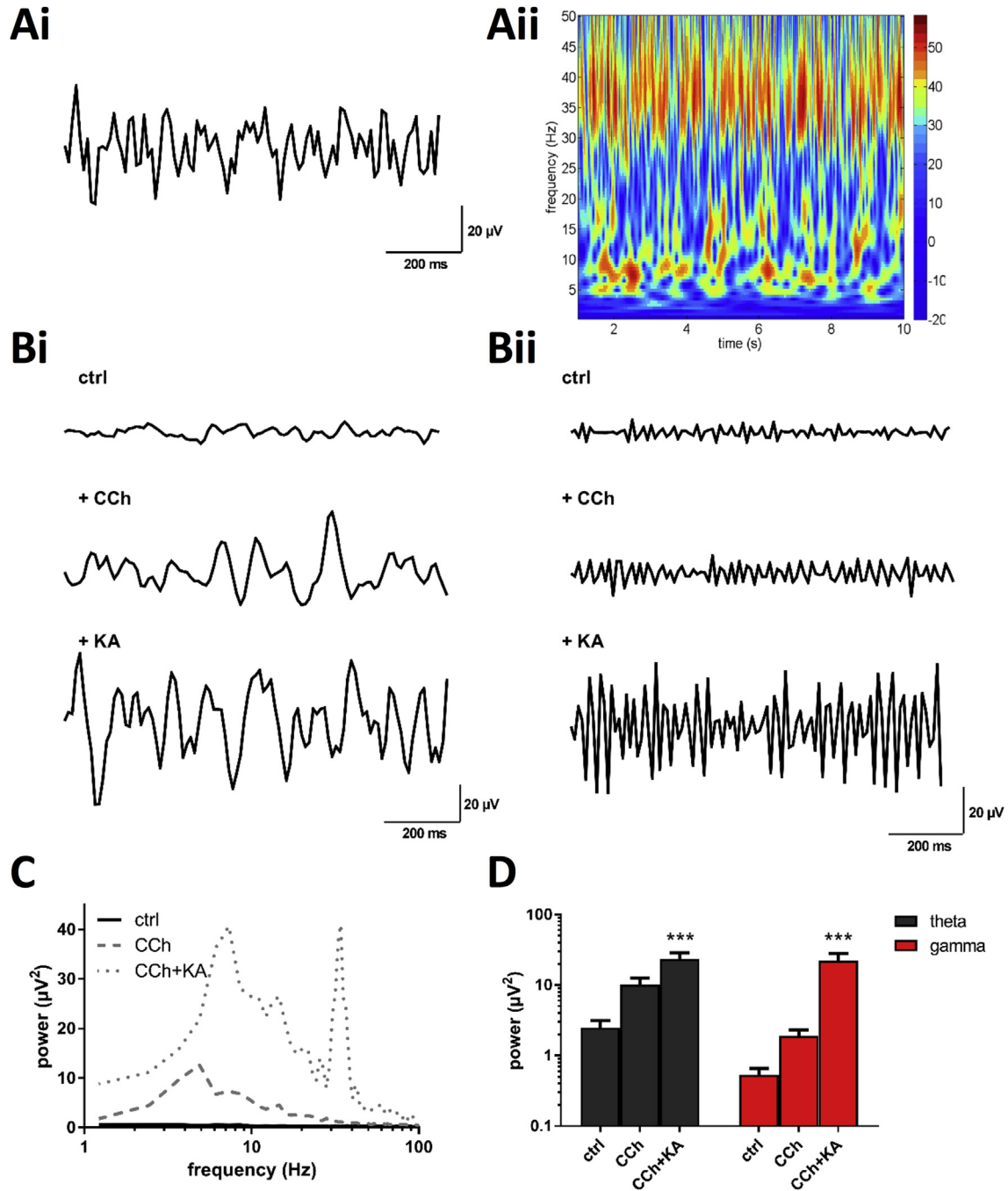
Fig. 1. Dual application of CCh and KA elicits simultaneous theta and gamma oscillations in layer V of M1.
(Ai) Data recorded in layer V of M1 following application of CCh (10 μM) and KA (150 nM) and low-pass filtered at 60 Hz (ii) a time-frequency spectrogram of data in Ai (Bi) Emergent theta activity filtered at 3–10 Hz and (ii) gamma activity filtered at 30–45 Hz following application of CCh and KA (C) Representative power spectra demonstrating emergence of theta and gamma oscillatory activity following application of CCh (dashed line) and subsequent addition of KA (dotted line). (D) Bar graphs showing peak oscillatory power of theta (grey bars) and gamma (red bars) oscillations normalised to control. ***p < 0.001.

and drug applied conditions. Unless otherwise stated pooled data are represented as mean peak power values normalised to control ± SEM. Statistical analyses performed were Wilcoxon matched-pairs signed rank test for all data except diazepam, gabazine, LY341495 and zolpidem where the Kruskal-Wallis test followed by Dunn's multiple comparisons test was performed to account for the consecutive concentrations of the drug tested. No significance is signified by "ns", whilst p < 0.05 is denoted by *, p < 0.01 by ** and p < 0.001 by ***. Significant changes in power and

frequency are given in a summary table (Table 1) with changes denoted by arrows (up represents increased frequency or power and down shows decrease. Number of arrows corresponds to significance at 1, 2 or 3*).

2.5. Modulation index (MI) and peak-triggered average analysis

Modulation index analyses were performed in Matlab (R2015b) by MathWorks. Analyses presented in Fig. 2 were performed on

Table 1
Summary of theta-gamma frequency and power changes in response to various ligands.

Drug		N (Slice)	Theta		Gamma	
			Frequency	Power	Frequency	Power
GABAergic receptors						
Gabazine	250 nM	7	–	↑	–	↓↓↓
	2 µM	7	↓↓	↑↑↑	↓↓	↓↓
Picrotoxin	50 µM	8	–	↑↑	↓↓	↓↓
Diazepam	30 µM	8	–	–	–	–
	100 µM	8	–	↑	↓	↑
Zolpidem	10 Nm	14	–	–	–	↑
	30 nM	14	–	–	↓	↑↑↑
	100 nM	8	–			
CGP55845	5 µM	17	↑↑	↑↑	↑↑	↑↑↑
Ionotropic glutamate receptors						
SYM 2206	20 µM	20	↓↓↓	↑↑↑	↓	↓↓↓
MK-801	20 µM	12	–	↑↑↑	↓↓↓	↑↑↑
Metabotropic glutamate receptors						
CPCCOEt	20 µM	7	–	↑	↓	↑
MTEP	100 µM	8	–	↑↑	–	↑↑
Cholinergic receptors						
Atropine	5 µM	7	–	↑	–	↑
Gap junctions						
Carbenoxolone	200 µM	13	↓↓	↓↓↓	–	↓↓↓

control data epochs that correspond to those used in subsequent figures and analyses. Measurement of Phase-amplitude coupling (PAC) to determine the modulation index of theta and gamma oscillations were performed using purpose built scripts previously described in Tort et al. (2010). Modulation index is presented as the mean ± SEM. In order to ensure robustness a high frequency peak-triggered average of the LFP was also constructed using a Matlab script supplied by B Polletta, based on the work of López-Azcárate et al. (2013). We set a threshold of MI > 0.0001 as evidence of coupling, and coupling was found in around 75% of slices tested.

3. Results

Recording in layer V of M1, application of CCh and KA generated simultaneous rhythms at theta frequency (6.6 ± 0.1 Hz, n = 169) and gamma frequency (36.6 ± 0.4 Hz, n = 169; Fig. 1Ai and Aii). Application of CCh (10 µM) resulted in a significant increase in neuronal activity at theta frequency (control mean peak power 2.50 ± 0.61 µV^2 versus 10.14 ± 2.43 µV^2 in CCh; n = 11, p < 0.05; Fig. 1B–D) and gamma frequency (control mean peak power 0.54 ± 0.13 µV^2 versus 1.89 ± 0.43 µV^2 in CCh; n = 11, p < 0.05; Fig. 1B–D). Subsequent addition of KA (150 nM) significantly increased the neuronal activity resulting in continuous oscillatory activity in the theta (mean peak power 23.48 ± 5.16 µV^2, n = 11, p < 0.001 compared to control; Fig. 1B–D) and gamma (22.17 ± 5.71 µV^2, n = 11, p < 0.001 compared to control; Fig. 1B–D) frequency ranges. Hence, co-application of both KA and CCh was required to reliably produce theta and gamma oscillations and was used for all further experiments. Interestingly, and as shown in the representative power spectrum in Fig. 1C, following addition of both KA and CCh we sometimes noted a peak in the low beta band (13–21 Hz) and a shift in peak theta frequency towards higher values. The latter
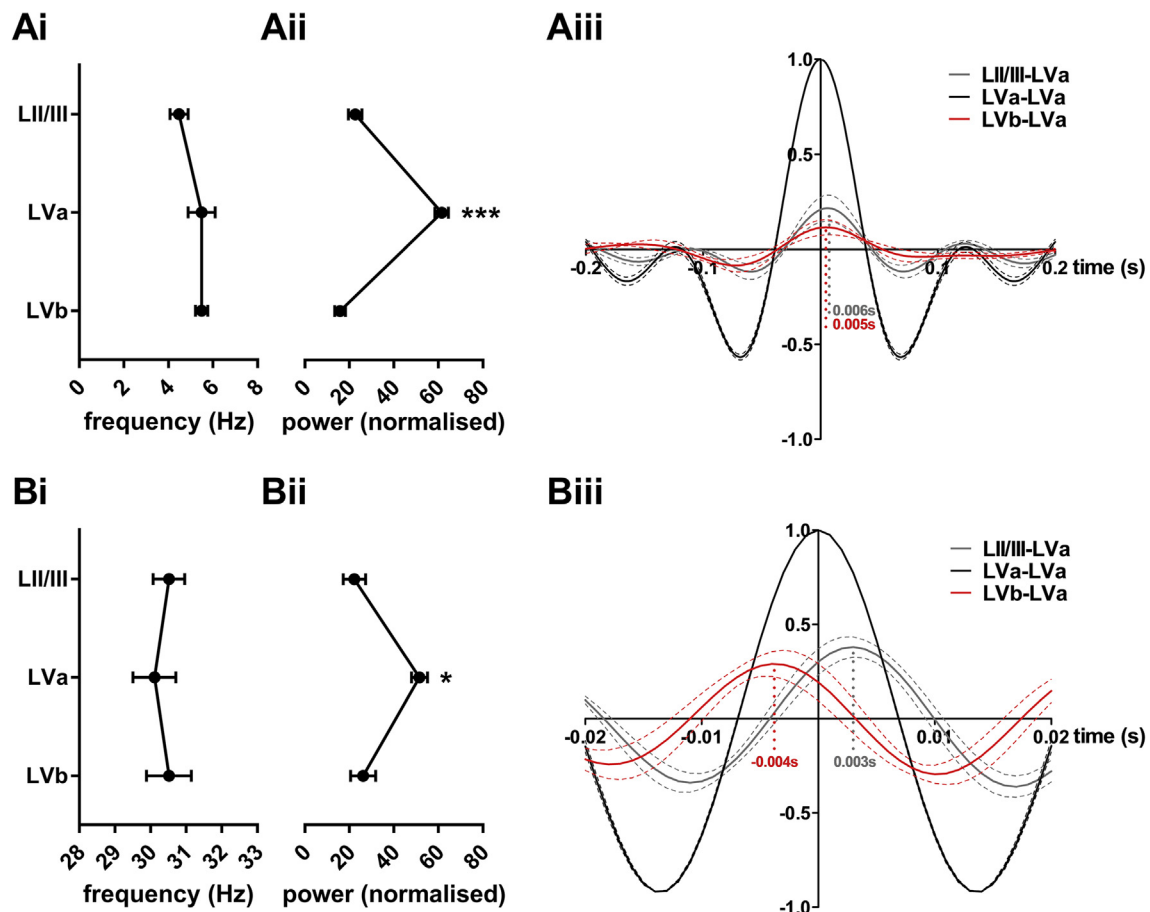

Fig. 2. Topography of theta-gamma oscillations across layers of M1.
Frequency (i) and power (ii) of (A) theta and (B) gamma oscillations from the superficial (layer II/III) to the deep (layer Vb) layers and (iii) cross-correlations demonstrating the lag time between layers.

effect was suggestive of development of a theta rhythm after application of KA that was in addition to the existing CCh-induced theta oscillation.

Previous work in our laboratory (Yamawaki et al., 2008) showed that the amplitude of beta oscillatory activity was greatest in deep layers of M1 and we next investigated the power of theta and gamma activity across cortical layers. On moving the recording electrode stepwise down from the pial surface of M1 towards the striatum, we found the power of both theta (Fig. 2Ai-ii) and gamma activity (Fig. 2Bi-ii) to be greatest in upper layer V. Hence, mean peak power for theta activity was 22.66 ± 3.03 μV^2 in layer II/III, compared to 61.49 ± 3.01 μV^2/Hz in layer Va and 15.85 ± 2.52 μV^2 in layer Vb (n = 6, p < 0.001, ANOVA). Similarly, for gamma activity mean peak power was 22.27 ± 5.01 μV^2 in layer II/III, compared to 51.52 ± 3.59 μV^2 in layer Va and 26.21 ± 5.58 μV^2 in layer Vb (n = 6, p < 0.05, ANOVA). However, cross-correlation analysis revealed a more complex relationship between oscillatory activity in different layers. As can be seen in Fig. 2Aiii, theta activity in deep M1 (layer Vb) lagged similar activity in layer Va (average lag 5 ms), as did activity in superficial M1 (average lag 6 ms). In both cases, correlation coefficients were low (LII/III versus LVa - 0.2164 ± 0.07 and LVb versus LVa - 0.11 ± 0.04). By contrast, in the case of gamma oscillations, the waveform in layer Va led layer Vb by an average of 4 ms and lagged superficial layers II/III by 3 ms. Correlation was much stronger across layers (LII/III versus LVa - 0.38 ± 0.05 LVb versus LVa - 0.29 ± 0.07). To further explore and understand the data we next investigated whether any interaction between the two rhythms could be detected.

The theta-gamma activity present in our *in vitro* preparation was the first such simultaneous persistent activity we have observed in this brain slice preparation, however, cross-frequency coupling has been shown many times *in vivo*. In order to confirm the existence of cross-frequency coupling in our data, we subjected time series data to further analyses. Recordings were analysed using the modulation index, based on the method of Tort et al. (2010), which offers a means of detecting PAC. The Tort et al. approach calculates how much an empirical amplitude distribution deviates from an ideal and produces a numerical output (the modulation index) which is a measure of the intensity of phase coupling. Although some recordings 14/54 slices (26%) showed no coupling above our threshold for detection (see methods), in many cases we were able to determine that theta-gamma oscillations in M1 were coupled (Fig. 3A–C; modulation index $2.28 \times 10^{-4} \pm 4.67 \times 10^{-5}$, n = 8). Similarly, we used the peak of the gamma oscillation waveform to trigger averaging of the theta oscillatory activity (Lopez-Azcarate et al., 2013; see methods), and this confirmed that packets of gamma activity were associated with the peak of the theta wave (Fig. 3D).

These analyses suggested that theta and gamma activity were coupled, and in order to provide further evidence of gamma and theta oscillations arising from separate neuronal networks a pharmacological dissection of mechanisms underlying the two oscillations was undertaken.

3.1. GABA receptor modulation of theta-gamma activity

Previous studies have shown that the oscillations in M1 are dependent on phasic $GABA_A$ receptor mediated inhibition (Yamawaki et al., 2008). Similarly, gamma oscillations have been shown to be exquisitely sensitive to blockade of $GABA_A$ receptor mediated inhibition by low concentrations of the competitive $GABA_A$ receptor antagonist, gabazine (250 nM). We tested gabazine at low (250 nM) and high (2 μM) concentration (Roopun et al., 2006) (Fig. 4A). At 250 nM gabazine significantly increased the power of theta oscillations ($147.9\pm 10.2\%$ of control, n = 7, p < 0.05)

while 2 μM gabazine shows an additional effect increasing the power by $181.0\pm 11.6\%$ of control, n = 7, p < 0.001 (Fig. 4 Ai, iii, iv). Both 250 nM and 2 μM gabazine substantially decreased the power of gamma oscillations (250 nM: $32.3\pm 4.9\%$ of control, n = 16, p < 0.001; 2 μM: $27.5\pm 7.5\%$ of control, n = 7, p < 0.01; Fig. 4Aii, iii, iv), indicating high sensitivity as previously reported for neocortical gamma activity. The effect of blocking $GABA_A$ receptors was confirmed using picrotoxin (Fig. 4B), which blocks the $GABA_A$ receptor ionophore. The application of 50 μM picrotoxin caused a similar decrease in gamma oscillatory power as seen with gabazine ($28.3\pm 7.4\%$ of control, n = 8, p < 0.01; Fig. 4Biv) and a significant increase in the power of theta oscillations ($239.8\pm 61.5\%$ of control, n = 8, p < 0.01; Fig. 4B i-iv).

We have previously shown that beta frequency oscillatory activity in M1 is sensitive to ligands which bind at the benzodiazepine site of the $GABA_A$ receptor, and we next explored the actions of benzodiazepine site ligands on theta and gamma activity. The benzodiazepine site agonist, diazepam, was initially applied at a concentration of 30 nM but there was no significant change in the power of theta or gamma oscillations at this concentration (theta: $174.0\pm 43.9\%$ of control, n = 8, ns; gamma: $121.9\pm 12.9\%$ of control, n = 8, ns; Fig. 5A). However at a concentration of 100 nM diazepam resulted in a significant increase in the power of both theta ($188.8\pm 26.1\%$ of control, n = 8, p < 0.05; Fig. 5Ai, iii, iv) and gamma oscillations ($142.2\pm 22.3\%$ of control, n = 8, p < 0.05; Fig. 5Aii, iii, iv).

Zolpidem is a non-benzodiazepine hypnotic which is specific for $GABA_A$ receptors containing the α_1-subunit at concentrations up to 400 nM (Crestani et al., 2000). When zolpidem was applied to theta oscillations there was no significant change at 10 and 30 nM concentrations (10 nM: $119.1\pm 6.0\%$ of control, n = 14, ns; 30 nM: $126.4\pm 10.1\%$ of control, n = 14, ns; Fig. 5Bi, iii, iv). However, increasing the concentration to 100 nM did result in a significant increase in power ($160.7\pm 16.0\%$ of control, n = 8, p < 0.001). In contrast, gamma oscillations increased in power upon addition of zolpidem, at all concentrations tested (10 nM: $148.5\pm 10.1\%$ of control, n = 14, p < 0.05; 30 nM: $87.1\pm 14.4\%$, n = 14, p < 0.001: 100 nM: $276.3\pm 28.0\%$ of control, n = 8, p < 0.001; Fig. 5Bii, iii, iv).

Finally, we investigated the involvement of $GABA_B$ receptor mediated inhibition in theta and gamma oscillations using the $GABA_B$ receptor antagonist, CGP55845, at 5 μM. Unlike the differing effects of the $GABA_A$ receptor antagonists, both theta and gamma oscillations showed significant increases in power in 5 μM CGP55845. Theta oscillations increased in power to $131.8\pm 10.6\%$ of control (n = 17, p < 0.01, Fig. 6Ai and B and C) and gamma oscillations increased in power to $149.4\pm 10.9\%$ of control (n = 17, p < 0.001, Fig. 6Aii, B and C). Application of CGP55845 also resulted in significant increases in both theta and gamma oscillatory frequencies (theta: to $119.1\pm 8.7\%$ of control, n = 17, p < 0.01; gamma: to $133.5\pm 10.3\%$ of control, n = 17, p < 0.01, data not shown).

3.2. Glutamate receptor modulation of theta-gamma activity

We next determined the role of excitatory glutamatergic transmission on coupled theta and gamma activity. Firstly, the role of AMPA receptors in the generation of theta and gamma oscillations was assessed using the antagonist SYM2206. SYM2206 (20 μM) significantly increased the power of the theta oscillations ($333.8\pm 20.2\%$ of control, n = 20, p < 0.001; Fig. 7Ai, iii, iv). In contrast, as with the blockade of $GABA_A$ receptors, SYM2206 (20 μM) dramatically decreased the power of gamma oscillations ($20.2\pm 3.2\%$ of control, n = 20, p < 0.001; Fig. 7Aii, iii, iv). It seems likely that the decrease in gamma activity and the increase in theta power are entirely separate mechanisms, however, it may be that SYM2206 merely depresses gamma frequency to the point where it is slow enough to contribute to an apparent increase in theta
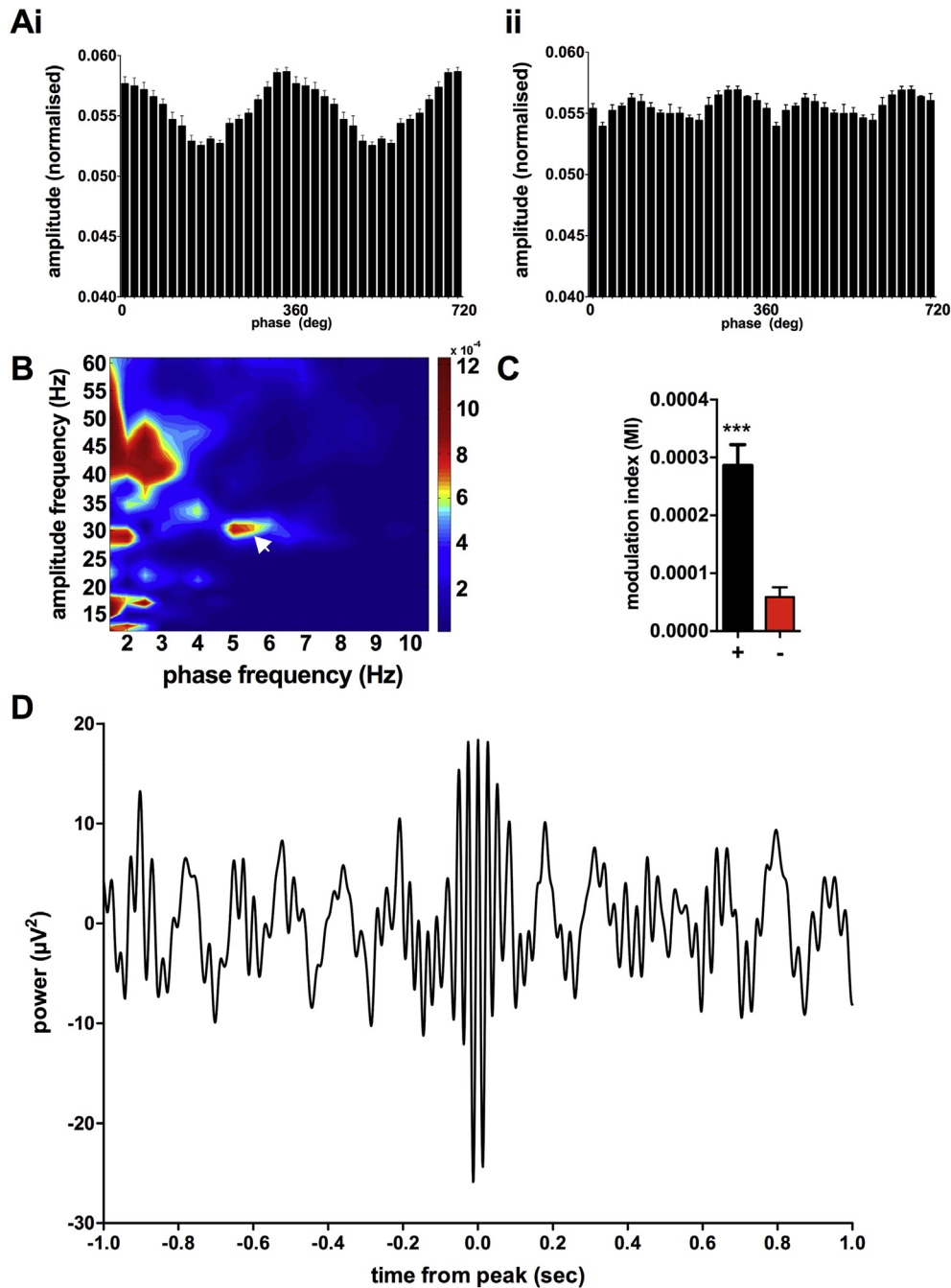
Fig. 3. Phase amplitude cross-frequency coupling and spike-triggered average analysis.
(A) Average phase angle representations of recordings (i) demonstrating theta-gamma PAC and (ii) those not demonstrating theta-gamma PAC. (B) Comodulogram demonstrating frequency pairs showing PAC (denoted by white arrow) (C) Bar graph demonstrating significant difference in modulation index (MI) between recordings showing PAC (+) and those not (−). (D) Representative spike-triggered average demonstrating gamma frequency oscillation at the peak of theta oscillation. ***, p < 0.001.

power. To investigate this, we measured the time course (data not shown) of the effects of SYM2206 on theta and gamma activity and it was notable that theta power peaked about 15 min prior to maximal depression of gamma activity, suggesting mechanistic independence. To assess the contribution of NMDA receptors we used the NMDA receptor non-competitive antagonist, ketamine, (20 μM), which increased theta to 146.6± 9.2% of control, n = 7, p < 0.05 and gamma: to 201.2± 23.6% of control, n = 7, p < 0.05, data not shown). Since ketamine may have non-NMDA receptor actions, we confirmed these data using another non-competitive NMDAR antagonist, MK-801. Application of MK-801 (20 μM) resulted in

significant increases in both theta and gamma oscillations (theta: 201.3± 22.5% of control, n = 12, p < 0.001; gamma: 254.7± 36.5% of control, n = 12, p < 0.001; Fig. 7Bi-iv). When we applied competitive NMDAR antagonists, we found gamma, but not theta activity to be augmented. Hence, when we applied 2-AP5 at 50 μM theta oscillations showed no significant change and gamma power was enhanced to 166.3± 13.6% of control, (n = 15, p < 0.001, data not shown) and similar experiments using the high affinity antagonist CPP (5 μM) again showed no significant change to theta power and increased gamma oscillatory power (179.5± 15.2% of control, n = 11, p < 0.01, data not shown).
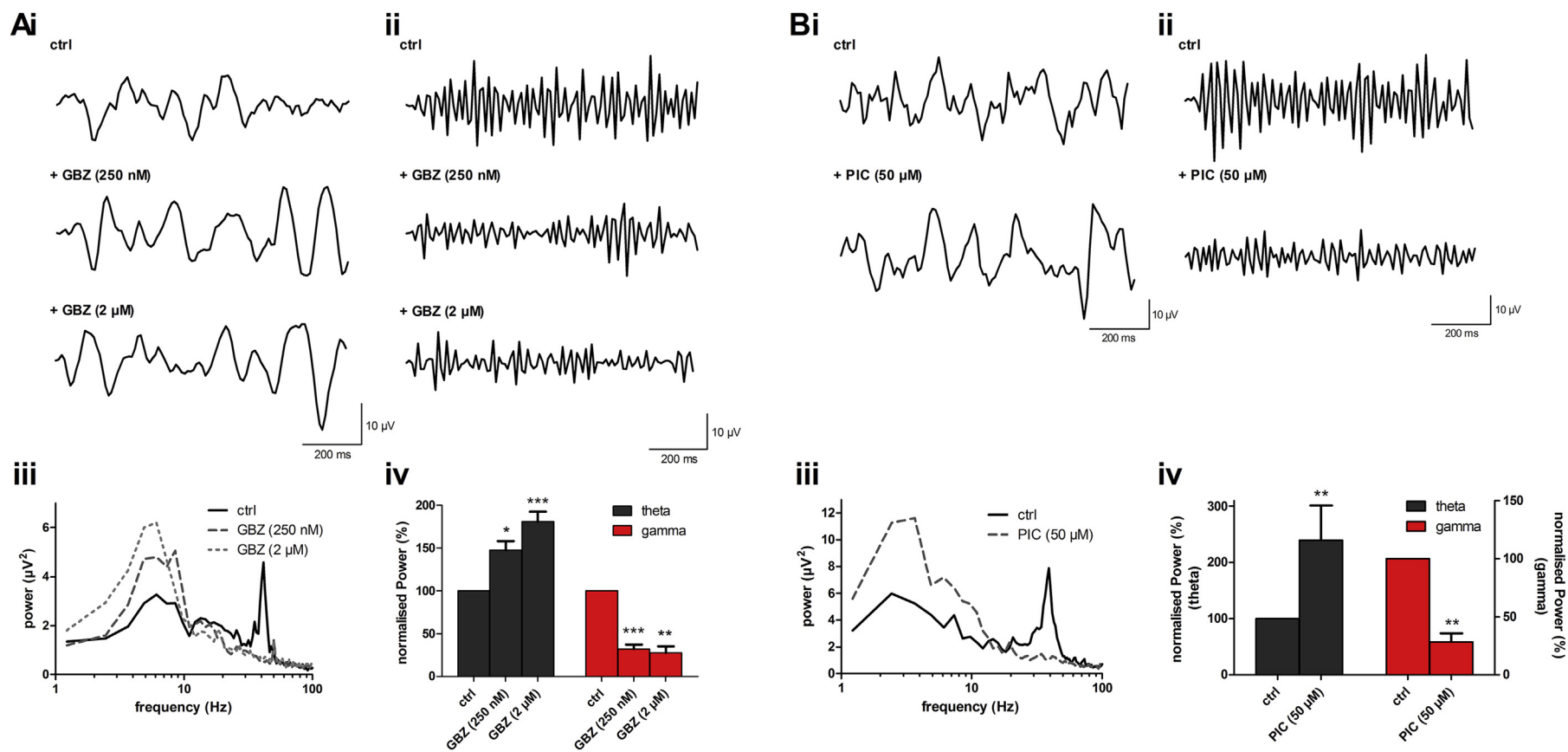
Fig. 4. GABA$_A$ receptor block increases theta oscillatory power whilst decreasing gamma oscillatory power.
(A) Effects of GABA$_A$ receptor antagonist gabazine (250 nM and 2 μM) on (i) theta and (ii) gamma oscillations. (iii) Representative power spectra showing peak power before (solid line) and after 250 nM (dashed line) and 2 μM (dotted line) gabazine. (iv) Bar graphs showing peak oscillatory power of theta (grey bars) and gamma (red bars) oscillations normalised to control. (B) Effect of the GABA$_A$ receptor channel blocker picrotoxin (50 μM) on (i) theta and (ii) gamma oscillations (iii) Representative power spectra demonstrating peak responses before (solid line) and after picrotoxin (dashed line) (iv) Bar graphs showing peak oscillatory power of theta (grey bars) and gamma (red bars) oscillations normalised to control. *p < 0.05 **p < 0.01, ***p < 0.001. (For interpretation of the references to colour in this figure legend, the reader is referred to the web version of this article.)
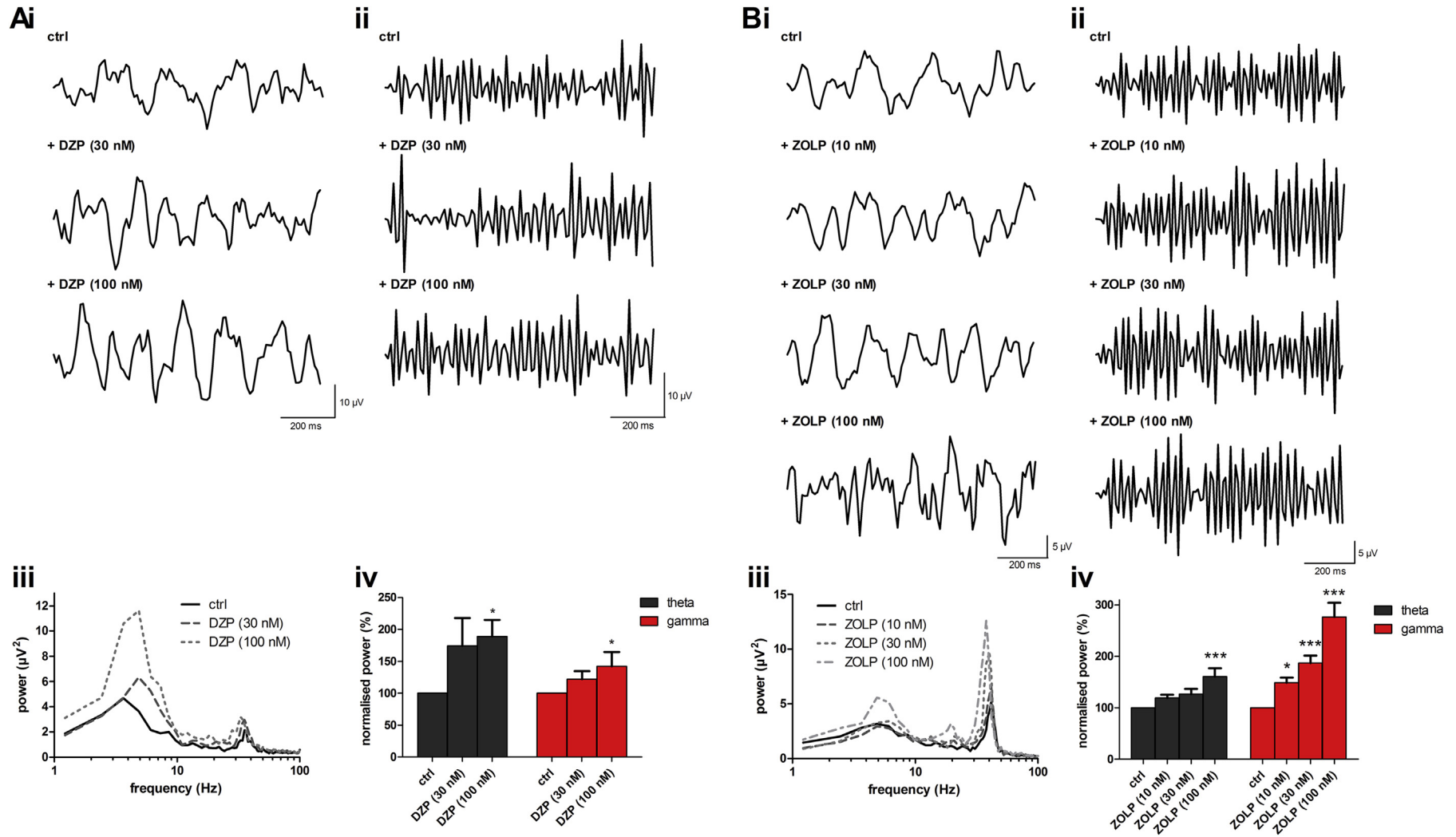
Fig. 5. Differential actions of benzodiazepine site modulation.
(A) Effects of diazepam (30 and 100 nM) on (i) theta and (ii) gamma oscillations (iii) Representative power spectra showing peak responses before (solid line) and after application of 30 nM (dashed line) and 100 nM (dotted line) diazepam. (iv) Bar graphs showing peak oscillatory power of theta (grey bars) and gamma (red bars) oscillations normalised to control. (B) Effects of zolpidem (10, 30 and 100 nM) on (i) theta and (ii) gamma oscillations (iii) Representative power spectra demonstrating peak responses before (solid line) and after application of 10 nM (dashed line), 30 nM (dotted line) and 100 nM (hybrid line) zolpidem. (iv) Bar graphs showing peak oscillatory power of theta (grey bars) and gamma (red bars) oscillations normalised to control. *p < 0.05 **p < 0.01, ***p < 0.001. (For interpretation of the references to colour in this figure legend, the reader is referred to the web version of this article.)
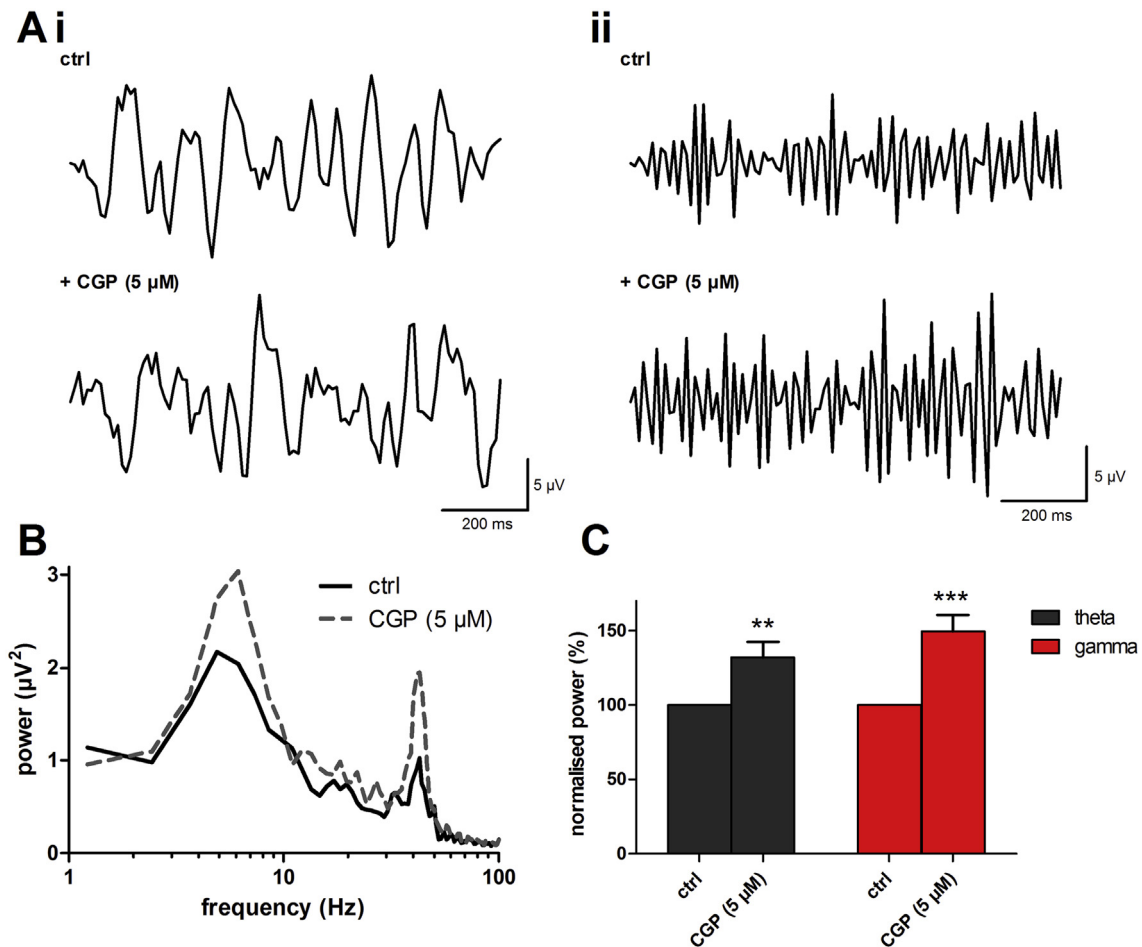
Fig. 6. GABA$_B$ receptor block increased both theta and gamma oscillatory power.
(A) Effects of GABA$_B$ receptor antagonist CGP55845 (CGP, 5 μM) on (i) theta and (ii) gamma oscillations. (B) Representative power spectra showing peak responses before (solid line) and after application of 5 μM (dashed line) CGP. (C) Bar graphs showing peak oscillatory power of theta (grey bars) and gamma (red bars) oscillations normalised to control. *p < 0.05 **p < 0.01, ***p < 0.001. (For interpretation of the references to colour in this figure legend, the reader is referred to the web version of this article.)

It is well established that activation of mGluRs may induce oscillatory activity *in vitro* (Whittington et al., 1995), and we next investigated the effect of antagonists for each of the group I mGluR subtypes to assess their involvement in theta and gamma oscillations in M1. We first blocked mGluR$_1$ receptors with the noncompetitive antagonist CPCCOEt. Application of CPCCOEt (20 μM) resulted in a significant increase in the power of both the theta and gamma oscillations (theta: 184.3± 22.5% of control, n = 7, p < 0.05; gamma: 216.1± 22.4% of control, n = 7, p < 0.05; Fig. 8A). When we applied MTEP (20 μM) in order to block mGluR$_5$ receptors, again this resulted in a significant increase in the power of both the theta and gamma oscillations such that theta power increased to 168.4± 18.5% of control, n = 8, p < 0.01 and gamma to 163.7± 10.8% of control, n = 8, p < 0.01 (Fig. 8B). By contrast, activation of group I mGluRs with the non-selective agonist, DHPG depressed theta power and had no significant effects on gamma activity (DHPG theta = 79.9± 4.0% of control, n = 10, p < 0.01 gamma = 89.6± 7.1% of control, n = 10, ns, data not shown).

3.3. Effects of other ligands on theta-gamma activity

Carbenoxolone has been used extensively to block gap junctions and has previously been shown to abolish beta oscillations in M1 (Yamawaki et al., 2008). Application of carbenoxolone (200 μM) for 90 min resulted in a significant decrease of both theta and gamma

oscillatory power (theta: 40.6± 5.1% of control, n = 13, p < 0.001; gamma: 28.7± 5.7% of control, n = 13, p < 0.001; Fig. 9A). The involvement of muscarinic acetylcholine receptors (mAChR) in both theta and gamma oscillations has been shown *in vivo* and through the use of CCh to induce oscillations in slices (Konopacki et al., 1987; Buhl et al., 1998; Fisahn et al., 1998; Lukatch and MacIver, 1997). Application of atropine (5 μM) completely abolished both theta (24.9± 9.0% of control, n = 7, p < 0.05, Fig. 9B) and gamma (9.1± 3.3% of control, n = 7, p < 0.05, Fig. 9B) oscillations.

4. Discussion

Using a modified slice preparation technique to enhance slice viability we have been able to generate simultaneous theta and gamma oscillations in sagittal slices of adult rat M1 using a pharmacological approach. These two rhythms are superficially similar to 'mu' and gamma activity we have reported in M1 *in vivo* using magnetoencephalography in human brain (MEG; Ronnqvist et al., 2013), although it is true to say that 'natural' M1 activity rarely has the power, or the sharply defined peaks seen in the *in vitro* brain slice. Presumably this reflects the difference between movement-elicited transient oscillatory activity *in vivo* and the strongly driven, persistent activity *in vitro*. The oscillations we report here show greatest power in layer V and appear to display cross-frequency coupling. M1 theta and gamma oscillations are
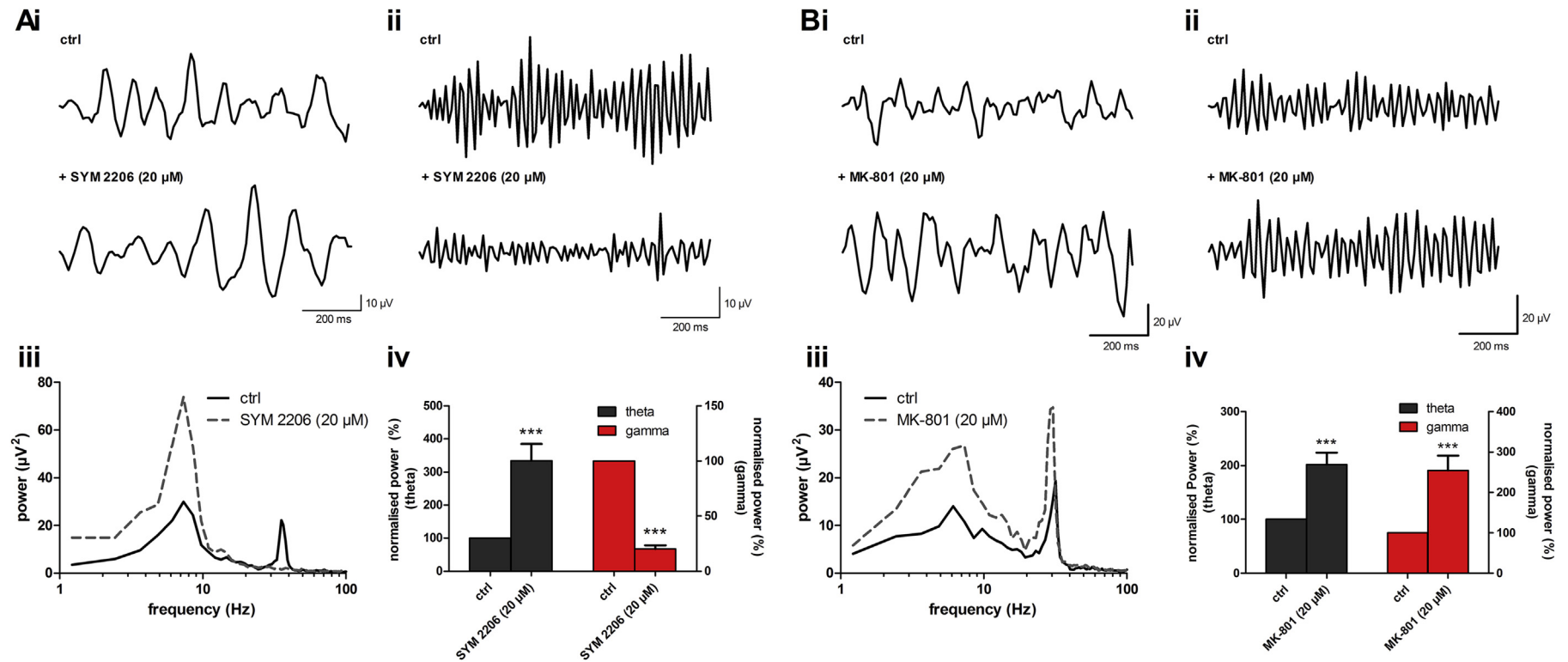
Fig. 7. AMPA receptor block increases theta power whilst reducing gamma power, whilst NMDA receptor block increased both theta and gamma oscillatory power.
(A) Effect of AMPA receptor antagonist SYM2206 (20 μM) on (i) theta and (ii) gamma oscillations (iii) Representative power spectra showing peak responses before (solid line) and after (dashed line) application of SYM2206. (iv) Bar graphs showing peak oscillatory power of theta (grey bars) and gamma (red bars) oscillations normalised to control. (B) Effect of the non-competitive NMDA receptor antagonist MK-801 (20 μM) on (i) theta and (ii) gamma oscillations. (iii) Representative power spectra demonstrating peak responses before (solid line) and after (dashed line) application of 20 μM MK-801. (iv) Bar graphs showing peak oscillatory power of theta (grey bars) and gamma (red bars) oscillations normalised to control. $^*p < 0.05$ $^{**}p < 0.01$, $^{***}p < 0.001$. (For interpretation of the references to colour in this figure legend, the reader is referred to the web version of this article.)
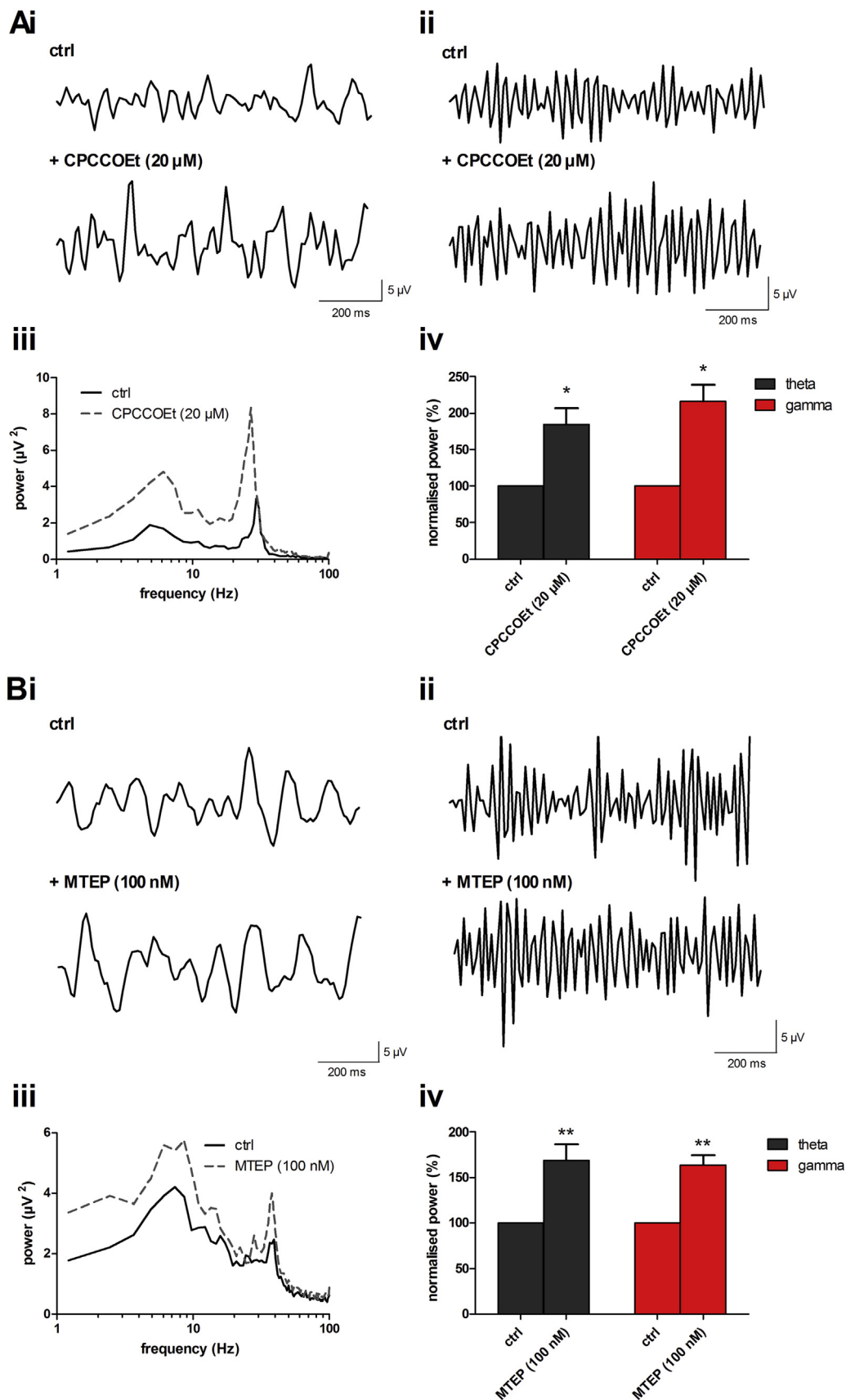
Fig. 8. **Blocking group I metabotropic glutamate receptors increases the power of theta and gamma oscillations in layer V of M1.** (A) Effect of the mGluR$_1$ antagonist CPCCOEt (20 μM) on (i) theta and (ii) gamma oscillations. (iii) Representative power spectra showing peak responses before (solid line) and after (dashed line) application of CPCCOEt. (iv) Bar graphs showing peak oscillatory power of theta (grey bars) and gamma (red bars) oscillations normalised to control. (B) Effect of mGluR$_5$ antagonist MTEP (100 nM) on (i) theta and (ii) gamma oscillations (iii) Representative power spectra demonstrating peak responses before (solid line) and after (dashed line) application of MTEP. (iv) Bar graphs showing peak oscillatory power of theta (grey bars) and gamma (red bars) oscillations normalised to control. $^*p < 0.05$ $^{**}p < 0.01$, $^{***}p < 0.001$. (For interpretation of the references to colour in this figure legend, the reader is referred to the web version of this article.)
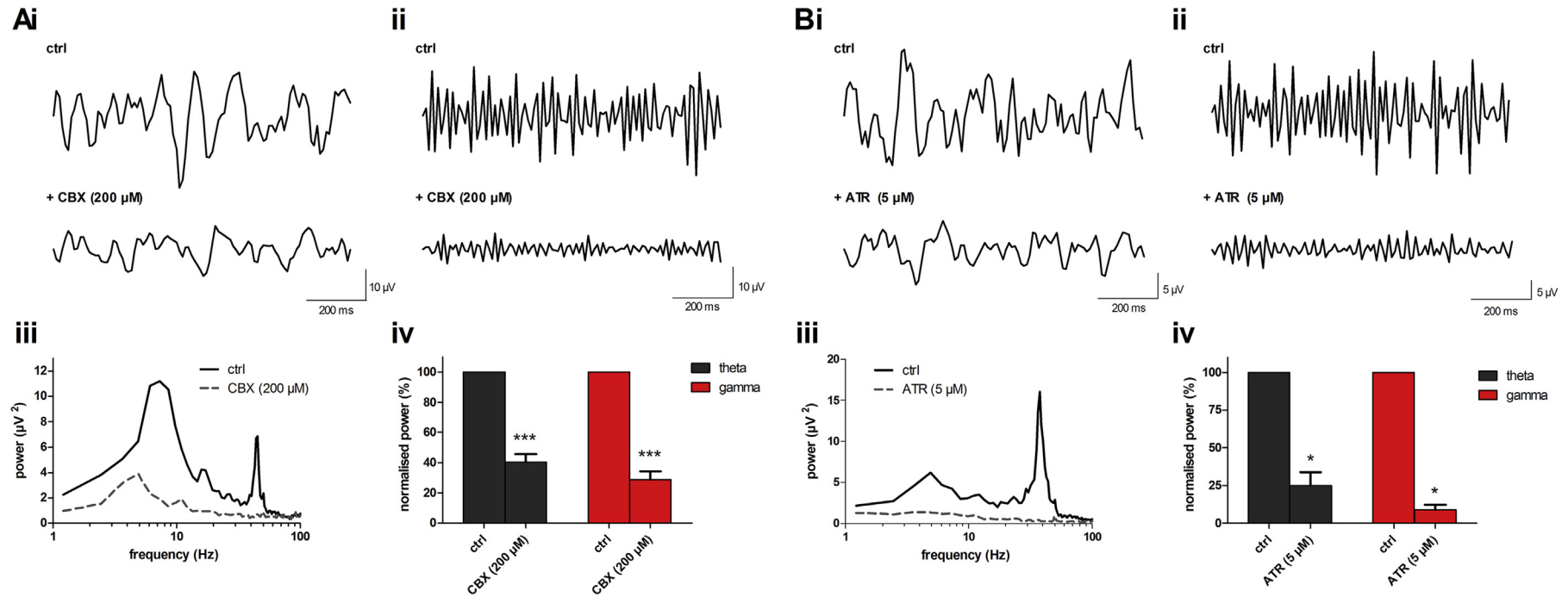
Fig. 9. Block of gap junctions and muscarinic acetylcholine receptors decreases power of theta and gamma oscillations.
(A) Effects of the gap junction blocker, carbenoxalone, (200 µM) on (i) theta and (ii) gamma oscillations. (iii) Associated power spectra demonstrating peak responses before (solid line) and after (dashed line) application of carbenoxolone. (iv) Bar graphs showing peak oscillatory power of theta (grey bars) and gamma (red bars) oscillations normalised to control. (B) Effects of the mAСh receptor blocker atropine (5 µM) on (i) theta and (ii) gamma oscillations. (iii) Associated power spectra demonstrating peak responses before (solid line) and after (dashed line) application of atropine. (iv) Bar graphs showing peak oscillatory power of theta (grey bars) and gamma (red bars) oscillations normalised to control. *p < 0.05 **p < 0.01, ***p < 0.001. (For interpretation of the references to colour in this figure legend, the reader is referred to the web version of this article.)

generated by discrete mechanisms, responding differentially to a range of pharmacological interventions at the major CNS excitatory and inhibitory receptors. Consistent with previous reports in cortex (e.g. Roopun et al., 2006), gamma activity was exquisitely sensitive to blockade of fast synaptic inhibition, but was also sensitive to gap junction block. Theta activity was much less sensitive to modulation of fast synaptic inhibition and excitation, suggesting a greater reliance on non-synaptic mechanisms. Further study of dual theta-gamma activity in the *in vitro* slice preparation has the potential to allow greater mechanistic understanding of how phase-amplitude coupling is mediated at the cellular and local network level, and how it is modulated by pharmacological manipulation.

4.1. KA and CCh generate simultaneous theta and gamma oscillations in layer V M1 in vitro

Co-application of KA and CCh has been used to generate gamma oscillations *in vitro* in hippocampus (Fisahn et al., 1998), somato-sensory cortex (Buhl et al., 1998; Roopun et al., 2006) and ento-rhinal cortex (Cunningham et al., 2003). We have previously used higher concentrations of KA and CCh (400 nM and 50 μM respectively) to generate beta oscillations in M1 (Yamawaki et al., 2008). However, in the present studies we have found that lower concentrations (100–150 nM kA and 5–10 μM CCh), are capable of producing multiple rhythms.

In relation to the novel observation of dual rhythms, we suspect that these differences are due to the improved viability of our M1 slice, and probably reflect better preservation of the GABA interneurons required for rhythmogenesis. As detailed in the Methods section above, we have utilised a number of 'neuro-protectant' agents during slice preparation, namely NAC, amino-guanidine, taurine, ethyl pyruvate and ascorbate, and these agents provided a step-change in slice viability and successful production of neuronal network oscillations in deep M1. When we performed immunocytochemistry for common interneuronal proteins such as parvalbumin (PV), calbindin and somatostatin, we did not observe a notable change in preservation of inhibitory cell somata compared to standard aCSF (data not shown), but we did see evidence of better dendritic preservation, though this is hard to quantify.

NAC has been shown to have neuroprotectant actions, restoring mitochondrial function in traumatic brain injury (Xiong et al., 1999) and increasing the pool of glutathione, a reactive oxygen species (ROS) scavenger (Chen et al., 2008; Ferrari et al., 1995). Amino-guanidine is a ROS scavenger associated with preventing apoptosis after ischemia (Dawson et al., 1993; Hunot et al., 1996; Sun et al., 2010). Taurine, a modulator of cytosolic and intra-mitochondrial calcium concentrations, can be employed to prevent mitochondrial death, and thus cell death, during traumatic events (Ellren and Lehmann, 1989). Similarly, cell volume regulation is a vital process (Inoue et al., 2005) and is regulated in part by taurine (Beetsch and Olson, 1998). Ascorbic acid, an important antioxidant and neuro-modulator is found at its highest concentration in the brain (Rice, 2000). It is found in CSF and extracellular fluid and is taken up by neurones where it is found at its highest concentration at 10 mM. Providing ascorbic acid in the modified aCSF means it can directly scavenge ROS and can be hetero-exchanged with glutamate, increasing levels in the extracellular fluid to minimise excitotox-icity. The standard aCSF solution used pyruvate in its salt form (sodium pyruvate). However, sodium pyruvate has been shown to be unstable and to dimerize rapidly into pyruvate hydrate and subsequently more slowly into parapyruvate, a compound that actually inhibits energy generation in neurones *in vitro* (Moyer et al., 2011; Zeng et al., 2007). Ethyl pyruvate, the ester form of pyruvic acid was thus used instead to help promote ATP generation. As ethyl pyruvate is lipophilic, it may penetrate into cells, where it can be hydrolysed by intracellular esterases to release pyruvate (Sims et al., 2001).

Taken together, these neuroprotectants combined in a modified aCSF solution have increased the preservation of neurons in M1 and also helped to increase number of slices that display neuronal network activity and show a definitive enhancement in slice viability.

4.2. Dependence of theta-gamma activity on excitatory and inhibitory synaptic transmission

Whilst their dependence on both KA and CCh may imply that the method of generation for both gamma and theta oscillations in M1 is similar, pharmacological characterisation reveals differences. Hence, gamma oscillatory power in M1 was significantly reduced by the GABA$_A$ antagonists gabazine and picrotoxin and the AMPA receptor blocker SYM2206 indicating dependence on recurrent excitatory and inhibitory synaptic transmission. By contrast theta oscillatory power was increased by block of either GABA$_A$ and AMPA receptors, consistent with a non-synaptically coupled network of oscillators in which synaptic blockade augments a non-synaptically generated rhythm (e.g. the beta 2 rhythm in somato-sensory cortex *in vitro* as shown by Roopun et al., 2006). Activation of the benzodiazepine site of the GABA$_A$ receptor with diazepam and zolpidem application resulted in increases in power of both theta and gamma oscillations, although the effect on theta rhythm is only observed at the highest concentrations of either drug. These data are consistent with the known synaptic inhibitory components of gamma oscillations, and suggest that the theta network may have a synaptic component as well as the previously discussed non-synaptic element and this may explain the shift in peak theta frequency seen between addition of CCh and subsequent addition of KA. The effects of benzodiazepine site agonists are suggestive of an increase in oscillatory power following recruitment and syn-chronous activation of pyramidal neurons, and may be related to the enhanced beta activity or 'beta buzz' seen *in vivo* (Glaze, 1990). Recent evidence suggests that a sustained inhibitory membrane conductance (I_{tonic}), arising from spill over of GABA, and mediated by high affinity extrasynaptic GABA$_A$ receptors (Bright et al., 2007; Farrant and Nusser, 2005) also plays a fundamental role in shaping network excitability (Mann and Mody, 2010; Semyanov et al., 2004) and this current is also present in M1, playing a role in beta oscil-latory activity (Prokic et al., 2015).

Blockade of NMDA receptors with NMDAR antagonists signifi-cantly increased power in both the theta and gamma band in M1, consistent with other reports of such NMDAR antagonist effects in the literature (Hakami et al., 2009; McNally et al., 2011; Pinault, 2008). It has been reported that GABA interneurons in hippocam-pal CA1 are highly sensitive to NMDAR antagonism (Grunze et al., 1996), and selective genetic ablation of NMDAR on parvalbumin positive (PV+) interneurons has been shown to augment gamma activity in the same region (Korotkova et al., 2010), with disinhi-bition of GABA interneurons being suggested as a mechanism for augmented excitability in pyramidal neurons, leading to increased oscillatory power. In the same study, Korotkova et al. (2010) showed selective interneuronal NMDAR ablation reduced theta power in CA1, an effect not seen in M1. This may reflect different local circuit organisation between hippocampus and neocortex, or simply be due to the acute versus chronic effects of ablation as compared to pharmacological intervention. Interestingly, the competitive antagonists, CPP and 2-AP5 did not affect theta power in our experiments, suggesting that NMDAR on GABA interneurons responsible for theta generation are not blocked at the concentra-tions used. The augmentation of theta power in hippocampus by NMDA antagonists contrasts with previous reports of theta power

reduction in CA1 (Gillies et al., 2002).

4.3. Gap junctions are required for both theta and gamma oscillations

Networks of inhibitory interneurons are known to be connected together by gap junctions, which allow them to provide large synchronous IPSPs to local excitatory cells involved in oscillations (Deans et al., 2001; Galarreta and Hestrin, 1999; Gibson et al., 1999). Pharmacological blockade of gap junction function with carbenoxolone, has been shown to abolish ultrafast oscillations (80–200 Hz, Draguhn et al., 1998) and gamma/beta oscillation *in vitro* (Cunningham et al., 2003; Deans et al., 2001; Roopun et al., 2006; Traub et al., 2000). Consistent with these observations, application of carbenoxolone, a gap junction channel blocker, here decreased and abolished theta and gamma oscillations respectively, confirming the essential nature of the inhibitory input provided by the interneuronal network.

4.4. mGluR mediated modulation of theta and gamma oscillations

Activation of mGluRs has in the past been shown to elicit gamma oscillations in hippocampus and neocortical slices via networks of interneurons (Whittington et al., 1995), reflecting the increase in network excitability seen in response to group I mGluR activation. Here we show that the addition of antagonists of group I mGluRs results in increased theta and gamma oscillatory power. Previous studies have reported that activation of group I mGluRs decreased synaptic inhibition (Desai and Conn, 1991; Varma et al., 2001) and it seems likely that blockade of mGluRs may result in increased synaptic inhibition, either through reduction in constitutive activity at the receptor or through reduction of glutamate driven activation of mGluRs in the KA/CCh activated network. In such a scenario, increased action-potential dependent GABA release may lead to increased oscillatory power in the same manner that positive modulation of GABA$_A$ receptors with benzodiazepines or barbiturates are known to do.

4.5. Theta-gamma cross-frequency coupling in M1

CFC (which includes PAC as well as many other forms of coupling) aids inter-network computational processing and communication and has been identified in behaving rats (Bragin et al., 1995; Buzsáki and Chrobak, 1995; Quilichini et al., 2010), monkeys (Lakatos et al., 2005) and in man (Mormann et al., 2005). CFC manifests between multiple brain regions in response to sensory inputs and cognitive or motor tasks and, as such, CFC is believed to be the primary mechanism by which brain areas and neuronal networks spatially and temporally co-ordinate activity (Gray et al., 1989; Jensen and Colgin, 2007). Igarashi et al. (2013) demonstrated the importance of theta and gamma oscillatory CFC in the sensorimotor area *in vivo*, suggesting that coupling between different ranges of gamma oscillations (high and low) was a dynamic system which could be attributed to different movement and behavioural states. To date, reports of CFC have been based on recordings made *in vivo* (Bragin et al., 1995; Chrobak and Buzsáki, 1998; Csicsvari et al., 2003; Mormann et al., 2005; Quilichini et al., 2010; Tort et al., 2008), and the current report is, to our knowledge, the first demonstration of CFC in an *in vitro* preparation of primary motor cortex.

Many studies have reported the importance of interneurons in generating synchronised IPSPs/IPSCs that contribute to the generation of gamma oscillations (e.g. Traub et al., 1996; Whittington et al., 1995). Similarly, mechanistic investigations in mouse hippocampal area CA1 *in vivo*, have shown specifically that coupling (and

not simply amplitude) of theta-gamma oscillations requires intact GABA inhibition onto PV + interneurons (Wulff et al., 2009). The coupled oscillatory activity we have reported here suggests that the relevant inhibitory networks in the M1 slice remain intact and that this preparation may prove useful for further mechanistic study of CFC *in vitro*.

5. Conclusions

These data show simultaneous theta and gamma oscillatory activity in layer V of M1 shows cross-frequency coupling and that the coupled rhythms are generated by different mechanisms.

References

Beetsch, J.W., Olson, J.E., 1998. Taurine synthesis and cysteine metabolism in cultured rat astrocytes: effects of hyperosmotic exposure. Am. J. Physiology-Cell Physiology 274, C866. C74.

Beierlein, M., Gibson, J.R., Connors, B.W., 2000. A network of electrically coupled interneurons drives synchronised inhibition in neocortex. Nat. Neurosci. 3 (9), 904–910.

Bocian, R., Posluszny, A., Kowalczyk, T., Kazmierska, P., Konopacki, J., 2011. Gap junction modulation of hippocampal formation theta and local cell discharges in anesthetized rats. Eur. J. Neurosci. 33, 471–481.

Bragin, A., Jando, G., Nadasdy, Z., Hetke, J., Wise, K., Buzsáki, G., 1995. Gamma (40-100-Hz) oscillation in the hippocampus of the behaving rat. J. Neurosci. 15, 47–60.

Bright, D.P., Aller, M.I., Brickley, S.G., 2007. Synaptic release generates a tonic GABA(A) receptor-mediated conductance that modulates burst precision in thalamic relay neurons. J. Neurosci. 27, 2560–2569.

Brown, P., Salenius, S., Rothwell, J.C., Hari, R., 1998. Cortical correlate of the piper rhythm in humans. J. Neurophysiol. 80, 2911–2917.

Buhl, E.H., Tamas, G., Fisahn, A., 1998. Cholinergic activation and tonic excitation induce persistent gamma oscillations in mouse somatosensory cortex in vitro. J. Physiol. 513, 117–126.

Buzsáki, G., Chrobak, J.J., 1995. Temporal structure in spatially organized neuronal ensembles - a role for interneuronal networks. Curr. Opin.Neurobiol. 5, 504–510.

Buzsáki, G., Moser, E.I., 2013. Memory, navigation and theta rhythm in the hippocampal-entorhinal system. Nat. Neurosci. 16 (2), 130–138.

Cacucci, F., Lever, C., Wills, T.J., Burgess, N., O'Keefe, J., 2004. Theta-modulated place-by-direction cells in the hippocampal formation in the rat. J. Neurosci. 24, 8265–8277.

Canolty, R.T., Edwards, E., Dalal, S.S., Soltani, M., Nagarajan, S.S., Kirsch, H.E., Berger, M.S., Barbaro, N.M., Knight, R.T., 2006. High gamma power is phase-locked to theta oscillations in human neocortex. Science 313, 1626–1628.

Cashdollar, N., Malecki, U., Rugg-Gunn, F.J., Duncan, J.S., Lavie, N., Duzel, E., 2009. Hippocampus-dependent and -independent theta-networks of active maintenance. Proc. Natl. Acad. Sci. (USA) 106 (48), 20493–20498.

Chen, G., Shi, J.X., Hu, Z.G., Hang, C.H., 2008. Inhibitory effect on cerebral inflammatory response following traumatic brain injury in rats: a potential neuroprotective mechanism of N-acetylcysteine. Mediat. Inflamm. 716458.

Cheyne, D., Bells, S., Ferrari, P., Gaetz, W., Bostan, A.C., 2008. Self-paced movements induce high-frequency gamma oscillations in primary motor cortex. Neuroimage 42, 332–342.

Chrobak, J.J., Buzsáki, G., 1998. Gamma oscillations in the entorhinal cortex of the freely behaving rat. J. Neurosci. 18, 388–398.

Cobb, S.R., Bulters, D.O., Davies, C.H., 2000. Coincident activation of mGluRs and mAChRs imposes theta frequency patterning on synchronised network activity in the hippocampal CA3 region. Neuropharmacology 39, 1933–1942.

Crestani, F., Martin, J.R., Mohler, H., Rudolph, U., 2000. Mechanism of action of the hypnotic zolpidem in vivo. Brit. J. Pharm. 131, 1251–1254.

Csicsvari, J., Jamieson, B., Wise, K.D., Buzsáki, G., 2003. Mechanisms of gamma oscillations in the hippocampus of the behaving rat. Neuron 37, 311–322.

Cunningham, M.O., Davies, C.H., Buhl, E.H., Kopell, N., Whittington, M.A., 2003. Gamma oscillations induced by kainate receptor activation in the entorhinal cortex in vitro. J. Neurosci. 23, 9761–9769.

Dawson, T.M., Dawson, V.L., Snyder, S.H., 1993. Nitric oxide as a mediator of neurotoxicity. NIDA Res. Monogr. 136, 258–271.

Deans, M.R., Gibson, J.R., Sellitto, C., Connors, B.W., Paul, D.L., 2001. Synchronous

activity of inhibitory networks in neocortex requires electrical synapses containing Connexin36. Neuron 31, 477–485.

Desai, M.A., Conn, P.J., 1991. Excitatory effects of ACPD receptor activation in the hippocampus are mediated by direct effects on pyramidal cells and blockade of synaptic inhibition. J. Neurophysiol. 66 (1), 40–52.

Dickson, C.T., Biella, G., de Curtis, M., 2000. Evidence for spatial modules mediated by temporal synchronization of carbachol-induced gamma rhythm in medial entorhinal cortex. J. Neurosci. 20, 7846–7854.

Draguhn, A., Traub, R.D., Schmitz, D., Jefferys, J.G.R., 1998. Electrical coupling underlies high-frequency oscillations in the hippocampus in vitro. Nature 394, 189–192.

Ellren, K., Lehmann, A., 1989. Calcium dependency of N-methyl-D-aspartate toxicity in slices from the immature rat hippocampus. Neuroscience 32, 371–379.

Engel, A.K., Singer, W., 2001. Temporal binding and the neural correlates of sensory awareness. Trends Cogn. Sci. 5, 16–25.

Farrant, M., Nusser, Z., 2005. Variations on an inhibitory theme: phasic and tonic activation of GABA(A) receptors. Nat. Rev. Neurosci. 6, 215–229.

Ferrari, G., Yan, C.Y., Greene, L.A., 1995. N-acetylcysteine (D- and L-stereoisomers) prevents apoptotic death of neuronal cells. J. Neurosci. 15, 2857–2866.

Fisahn, A., Pike, F.G., Buhl, E.H., Paulsen, O., 1998. Cholinergic induction of network oscillations at 40 Hz in the hippocampus in vitro. Nature 394, 186–189.

Galarreta, M., Hestrin, S., 1999. A network of fast-spiking cells in the neocortex connected by electrical synapses. Nature 402, 72–75.

Gibson, J.R., Beierlein, M., Connors, B.W., 1999. Two networks of electrically coupled inhibitory neurons in neocortex. Nature 402, 75–79.

Gillies, M.J., Traub, R.D., LeBeau, F.E.N., Davies, C.H., Gloveli, T., Buhl, E.H., Whittington, M.A., 2002. A model of atropine-resistant theta oscillations in rat hippocampal area CA1. J. Physiol. 543, 779–793.

Glaze, D.G., 1990. Drug effects. In: Daly, D.D., Pedley, T.A. (Eds.), Current Practice of Clinical Electro- Encephalography, second ed. Raven Press, New York, pp. 489–512.

Gray, C.M., 1994. Synchronous oscillations in neuronal systems: mechanisms and functions. J. Comput. Neurosci. 1, 11–38.

Gray, C.M., Konig, P., Engel, A.K., Singer, W., 1989. Oscillatory responses in cat visual-cortex exhibit inter-columnar synchronization which reflects global stimulus properties. Nature 338, 334–337.

Griffiths, M.J.D., Messent, M., Macallister, R.J., Evans, T.W., 1993. Aminoguanidine selectively inhibits inducible nitric-oxide synthase. Brit J. Pharm 110, 963–968.

Grunze, H.C., Rainnie, D.G., Hasselmo, M.E., Barkai, E., Hearn, E.F., McCarley, R.W., Greene, R.W., 1996. NMDA-dependent modulation of CA1 local circuit inhibition. J. Neurosci. 16, 2034–2043.

Hakami, T., Jones, N.C., Tolmacheva, E.A., Gaudias, J., Chaumont, J., Salzberg, M., O'Brien, T.J., Pinault, D., 2009. NMDA receptor hypofunction leads to generalized and persistent aberrant gamma oscillations independent of hyperlocomotion and the state of consciousness. PLoS One 4, e6755.

Hunot, S., Boissiere, F., Faucheux, B., Brugg, B., Mouatt-Prigent, A., Agid, Y., Hirsch, E.C., 1996. Nitric oxide synthase and neuronal vulnerability in Parkinson's disease. Neuroscience 72, 355–363.

Igarashi, J., Isomura, Y., Arai, K., Harukuni, R., Fukai, T., 2013. A theta-gamma oscillation code for neuronal coordination during motor behavior. J. Neurosci. 33, 18515–18530.

Inoue, H., Mori, S., Morishima, S., Okada, Y., 2005. Volume-sensitive chloride channels in mouse cortical neurons: characterization and role in volume regulation. Eur. J. Neurosci. 21, 1648–1658.

Jensen, O., Colgin, L.L., 2007. Cross-frequency coupling between neuronal oscillations. Trends Cognitive Sci. 11, 267–269.

Konopacki, J., Golebiewski, H., 1993. Theta-like activity in hippocampal-formation slices - cholinergic-GABAergic interaction. Neuroreport 4, 963–966.

Konopacki, J., Maciver, M.B., Bland, B.H., Roth, S.H., 1987. Carbachol-induced EEG theta-activity in hippocampal brain-slices. Brain Res. 405, 196–198.

Kopell, N., Ermentrout, B., 2004. Chemical and electrical synapses perform complementary roles in the synchronization of interneuronal networks. Proc. Natl. Acad. Sci. (USA) 01, 15482–15487.

Korotkova, T., Fuchs, E.C., Ponomarenko, A., von Engelhardt, J., Monyer, H., 2010. NMDA receptor ablation on parvalbumin-positive interneurons impairs hippocampal synchrony, spatial representations, and working memory. Neuron 68, 557–569.

Lacey, M.G., Gooding-Williams, G., Prokic, E.J., Yamawaki, N., Hall, S.D., Stanford, I.M., Woodhall, G.L., 2014. Spike firing and IPSPs in Layer V pyramidal neurons during beta oscillations in rat primary motor cortex (M1) in vitro. Plos One 9 (1), e85109.

Lakatos, P., Shah, A.S., Knuth, K.H., Ulbert, I., Karmos, G., Schroeder, C.E., 2005. An oscillatory hierarchy controlling neuronal excitability and stimulus processing in the auditory cortex. J. Neurophysiol. 94, 1904–1911.

Lisman, J.E., Idiart, M.A.P., 1995. Storage of 7+/-2 short-term memories in oscillatory subcycles. Science 267, 1512–1515.

Lopez-Azcarate, J., Nicolas, M.J., Cordon, I., Alegre, M., Valencia, M., Artieda, J., 2013. Delta-mediated cross-frequency coupling organizes oscillatory activity across the rat cortico-basal ganglia network. Front. Neural Circuits 2 (7), 155.

Lukatch, H.S., MacIver, M.B., 1997. Physiology, pharmacology, and topography of cholinergic neocortical oscillations in vitro. J. Neurophysiol. 77, 2427–2445.

MacIver, M.B., Harris, D.P., Konopacki, J., Roth, S.H., Bland, B.H., 1986. Carbachol induced rhythmical slow wave activity recorded from dentate granule neurons in vitro. Proc. West Pharmacol. Soc. 29, 159–161.

Mann, E.O., Mody, I., 2010. Control of hippocampal gamma oscillation frequency by tonic inhibition and excitation of interneurons. Nat. Neurosci. 13, 205–221.

McNally, J.M., McCarley, R.W., McKenna, J.T., Yanagawa, Y., Brown, R.E., 2011. Complex receptor mediation of acute ketamine application on in vitro gamma oscillations in mouse prefrontal cortex, Modeling gamma band oscillation abnormalities in schizophrenia. Neuroscience 199, 51–63.

Mormann, F., Fell, J., Axmacher, N., Weber, B., Lehnertz, K., Elger, C.E., Fernández, G., 2005. Phase/amplitude reset and theta-gamma interaction in the human medial temporal lobe during a continuous word recognition memory task. Hippocampus 15, 890, 90.

Moyer Jr., J.R., Furtak, S.C., McGann, J.P., Brown, T.H., 2011. Aging-related changes in calcium-binding proteins in rat perirhinal cortex. Neurobiol. Aging 32, 1693–1706.

Muthukumaraswamy, S.D., 2010. Functional properties of human primary motor cortex gamma oscillations. J. Neurophysiol. 104, 2873–2885.

O'Keefe, J., Recce, M.L., 1993. Phase relationship between hippocampal place units and the EEG theta-rhythm. Hippocampus 3, 317–330.

Pakhotin, P.I., Pakhotina, I.D., Andreev, A.A., 1997. Functional stability of hippocampal slices after treatment with cyclooxygenase inhibitors. Neuroreport 8, 1755–1759.

Pálmalmi, J., Paulsen, O., Freund, T.F., Hájos, N., 2004 Sep. Distinct properties of carbachol- and DHPG-induced network oscillations in hippocampal slices. Neuropharmacology 47 (3), 381–389. PubMed PMID: 15275827.

Pfurtscheller, G., Graimann, B., Huggins, J.E., Levine, S.P., Schuh, L.A., 2003. Spatiotemporal patterns of beta desynchronization and gamma synchronization in corticographic data during self-paced movement. Clin. Neurophysiol. 114, 1226–1236.

Pinault, D., 2008. N-methyl d-aspartate receptor antagonists ketamine and MK-801 induce wake-related aberrant gamma oscillations in the rat neocortex. Biol. Psychiatry 63, 730–735.

Proctor, P.H., 2008. Uric acid and neuroprotection. Stroke 39, E126. E126.

Prokic, E.J., Weston, C., Yamawaki, N., Hall, S.D., Jones, R.S., Stanford, I.M., Ladds, G., Woodhall, G.L., 2015. Cortical oscillatory dynamics and benzodiazepine-site modulation of tonic inhibition in fast spiking interneurons. Neuropharmacology 95, 192–205.

Quilichini, P., Sirota, A., Buzsáki, G., 2010. Intrinsic circuit organization and theta-gamma oscillation dynamics in the entorhinal cortex of the rat. J. Neurosci. 30, 11128–11142.

Rice, M.E., 2000. Ascorbate regulation and its neuroprotective role in the brain. Trends Neurosci. 23, 209–216.

Ronnqvist, K.C., McAllister, C.J., Woodhall, G.L., Stanford, I.M., Hall, S.D., 2013. A multimodal perspective on the composition of cortical oscillations. Front. Hum. Neurosci. 7, 132.

Roopun, A.K., Middleton, S.J., Cunningham, M.O., LeBeau, F.E.N., Bibbig, A., Whittington, M.A., Traub, R.D., 2006. A beta2-frequency (20-30 Hz) oscillation in nonsynaptic networks of somatosensory cortex. Proc. Natl. Acad. Sci. U. S. A. 103, 15646–15650.

Semyanov, A., Walker, M.C., Kullmann, D.M., 2004. Tonically active GABA A receptors: modulating gain and maintaining the tone. Trends Neurosci. 27, 262–269.

Sims, C.A., Wattanasirichaigoon, S., Menconi, M.J., Ajami, A.M., Fink, M.P., 2001. Ringer's ethyl pyruvate solution ameliorates ischemia/reperfusion-induced intestinal mucosal injury in rats. Crit. Care Med. 29, 1513–1518.

Singer, W., Gray, C.M., 1995. Visual feature integration and the temporal correlation hypothesis. Ann. Rev. Neurosci. 18, 555–586.

Sirota, A., Montgomery, S., Fujisawa, S., Isomura, Y., Zugaro, M., Buzsáki, G., 2008. Entrainment of neocortical neurons and gamma oscillations by the hippocampal theta rhythm. Neuron 60, 683–697.

Sun, M., Zhao, Y., Gu, Y., Xu, C., 2010. Neuroprotective actions of aminoguanidine involve reduced the activation of calpain and caspase-3 in a rat model of stroke. Neurochem. Int. 56, 634–641.

Szabadics, J., Lorincz, A., Tamas, G., 2001. Β and γ frequency synchronization by dendritic gabaergic synapses and gap junctions in a network of cortical interneurons. J. Neurosci. 21 (15), 5824–5831.

Tamas, G., Buhl, E.H., Lorincz, A., Somogyi, P., 2000. Proximally targeted GABAergic synapses and gap junctions synchronise cortical interneurons. Nat. Neurosci. 3, 366–371.

Tort, A.B.L., Kramer, M.A., Thorn, C., Gibson, D.J., Kubota, Y., Graybiel, A.M., Kopell, N.J., 2008. Dynamic cross-frequency couplings of local field potential oscillations in rat striatum and hippocampus during performance of a T-maze task. Proc. Natl. Acad. Sci. (USA) 105, 20517–20522.

Tort, A.B.L., Komorowski, R., Eichenbaum, H., Kopell, N., 2010. Measuring phase-amplitude coupling between neuronal oscillations of different frequencies. J. Neurophysiol. 104, 1195–1210.

Traub, R.D., Whittington, M.A., Colling, S.B., Buzsáki, G., Jefferys, J.G.R., 1996. Analysis of gamma rhythms in the rat hippocampus in vitro and in vivo. J. Physiol. 493, 471–484.

Traub, R.D., Bibbig, A., Fisahn, A., LeBeau, F.E.N., Whittington, M.A., Buhl, E.H., 2000. A model of gamma-frequency network oscillations induced in the rat CA3 region by carbachol in vitro. Eur.J. Neurosci. 12, 4093–4106.

Varma, N., Carlson, G.C., Ledent, C., Alger, B.E., 2001. Metabotropic glutamate receptors drive the endocannabinoid system in hippocampus. J. Neurosci. 21, RC188.

Wang, X.-J., Buzsáki, G., 1996. Gamma oscillation by synaptic inhibition in a hippocampal interneuronal network model. J. Neurosci. 16, 6402–6413.

Whittington, M.A., Traub, R.D., Jefferys, J.G.R., 1995. Synchronised oscillations in

interneuron networks driven by metabotropic glutamate-receptor activation. Nature 373, 612–615.

Whittington, M.A., Traub, R.D., Faulkner, H.J., Stanford, I.M., Jefferys, J.G.R., 1997. Recurrent excitatory postsynaptic potentials induced by synchronised fast cortical oscillations. Proc. Natl. Acad. Sci. (USA) 94, 12198–12203.

Wulff, P., Ponomarenko, A.A., Bartos, M., Korotkova, T.M., Fuchs, E.C., Bähner, F., Both, M., Tort, A.B.L., Kopell, N.J., Wisden, W., Monyer, H., 2009. Hippocampal theta rhythm and its coupling with gamma oscillations require fast inhibition onto parvalbumin-positive interneurons. Proc. Natl. Acad. Sci. (USA) 106,

3561–3566.

Xiong, Y., Peterson, P.L., Lee, C.P., 1999. Effect of N-acetylcysteine on mitochondrial function following traumatic brain injury in rats. J. Neurotrauma 16, 1067–1082.

Yamawaki, N., Stanford, I.M., Hall, S.D., Woodhall, G.L., 2008. Pharmacologically induced and stimulus evoked rhythmic neuronal oscillatory activity in the primary motor cortex in vitro. Neuroscience 151, 386–395.

Zeng, J., Liu, J., Yang, G.Y., Kelly, M.J., James, T.L., Litt, L., 2007. Exogenous ethyl pyruvate versus pyruvate during metabolic recovery after oxidative stress in neonatal rat cerebrocortical slices. Anesthesiology 107, 630–640.